Effects of variogram characteristics of coal permeability on CBM production: a case study in Southeast Qinshui Basin, China

Fengde Zhou[1,2*], Guangqing Yao[1] and Jianzhong Wang[3]

[1]Key Laboratory of Tectonics and Petroleum Resources (China University of Geosciences), Ministry of Education, Wuhan 430074, China

[2]School of Petroleum Engineering, University of New South Wales, Sydney, NSW 2052, Australia

[3]China United Coalbed Methane Corporation Ltd. Jincheng, Shanxi 048000, China

**Corresponding author. Email: fdzhou@cug.edu.cn; f.zhou@unsw.edu.au*

(Received 26 April 2013; accepted 22 November 2013)

Abstract

The coalbed methane (CBM) resources of China are located mainly in 9 basins, Ordos, Qinshui, Jungar, Diandongqianxi, Erlian, Tuha, Tarim, Tianshan and Hailaer. Qinshui Basin, one of the richest CBM basins in China, has boosted its annual CBM production to 3×10^9 m^3 (106 Bcf). The coal seams in Qinshui Basin are significant with high gas content but strong heterogeneous permeabilities ranging from 0.1 to 10 mD. This paper investigates the effects of spatial distribution characteristics of coal permeability on CBM production. The study area is the South Shizhuang CBM district, Southeast of Qinshui Basin. The distributions of porosity, ash content, coal density and gas content of the coal seam are generated using sequential Gaussian simulation (SGS) with only one realisation because this paper only justifies the effects of coal permeability on CBM production. The permeabilities of 17 wells are determined by matching these wells' water and gas production with bottom-hole pressure as constraint. Then, the distributions of coal permeabilities are generated using SGS with a commercial simulator. The history matched permeabilities range from 1.5 to 12 mD with average of 2.9 mD of the 17 wells. Eight variogram models are used to build the distributions of permeability. The cumulative gas productions of two different well-spacing cases, 300 m and 2000 m, are compared. There are 20 realisations of permeability for each of the eight models. The results show that historical matching can be used to obtain the porosity multipliers and the permeabilities in wells. The major direction of variogram has less effect on the uncertainty of field CBM production than variogram range. The effects of variogram range on the uncertainty of CBM production are positive for the case with short well spacing and vice versa for the case with long well spacing.

Keywords: History matching, Variogram characteristics, CBM production

1. INTRODUCTION

Coal seams in the Qinshui Basin have relatively low permeability, ranging from 0.1-10×10^{-15} m^2 (0.1- 10 mD; Stevens *et al*., 1998; Keim *et al*., 2011). Our experimental data show that the coal seam permeability is low as 3×10^{-17} m^2 (0.03 mD) and sensitive to effective stress. The strong heterogeneous coal permeability has strong effects on water and gas production. Estimation of CBM production is crucial for planning and designing of CBM field. The estimation is highly uncertain due to the lack of enough data between wells, especially at the beginning of the CBM production. Hence, the uncertainty involved in predicting the CBM production must be assessed. Coal permeability, coal porosity, coal density and coal gas content are mentioned to be four major parameters that introduce the uncertainty in CBM production.

In South Shizhuang CBM field, some wells experienced high water production initially, but without gas production (Lv *et al*., 2012), while some wells produced gas earlier after decades days of dewatering. Numerical reservoir simulator which accounts for the various mechanism was considered as an efficient technique to analyse the production behaviours and predict the future CBM production (Zhou, 2012), instead of the conventional reservoir engineering techniques. Numerical simulation also allows us to predict the permeability, skin factor, saturation, etc. using history data. However, a given history matching is not unique. We can obtain similar matches using different combinations of input data (Zhou, 2012). If possible, this must be minimized by integrating all available data.

There are many geological parameters which affect the CBM production, e.g. coal thickness, porosity, permeability, relative permeability (Ding *et al*., 2012). An appropriate geological model with spatial distributions of the parameters can improve the reliability of CBM production prediction. Geostatistics was used to estimate the distributions of coal thickness (Jakeman, 1980; Mastalerz and Kenneth, 1994; Zhou *et al*., 2012), coal quality (Cairncross and Cadle, 1988; Hagelskamp *et al*., 1988; Liu *et al*., 2005; Heriawan and Koike, 2008; Beretta *et al*., 2010; Hindistan *et al*., 2010) and coal properties. These distributions can be used to assess the uncertainty in CBM production. The coal thickness can be determined from drilling and log data. The coal porosity and permeability can be estimated by history matching using numerical simulation. The adsorption data are sourced from experiments. The distribution of these parameters can then be predicted using a geostatistical method such as SGS and ordinary kriging (Beretta *et al*., 2010).

In this paper, 24 wells are simulated separately in 6 pilots, but 7 wells of them are not history matched because they have no gas production. Therefore, we history matched the gas and water production rate and bottom-hole pressure (BHP) with the field data from 17 wells using a commercial simulator by changing the porosity, permeability and skin factor of the coal seam. Then, the history matched permeabilities of the 17 wells are used to populate the permeability distributions with different variogram models using SGS. The cumulative CBM productions of the different permeability distribution models were compared using numerical simulation method.

The stratigraphy of the study area was divided into three systems (Ordovician, Carboniferous and Permian) and five groups (Fengfeng, Benxi, Taiyuan, Shanxi and Low Shihezhi) from bottom to top (Figure 1). The currently producing coal seam is

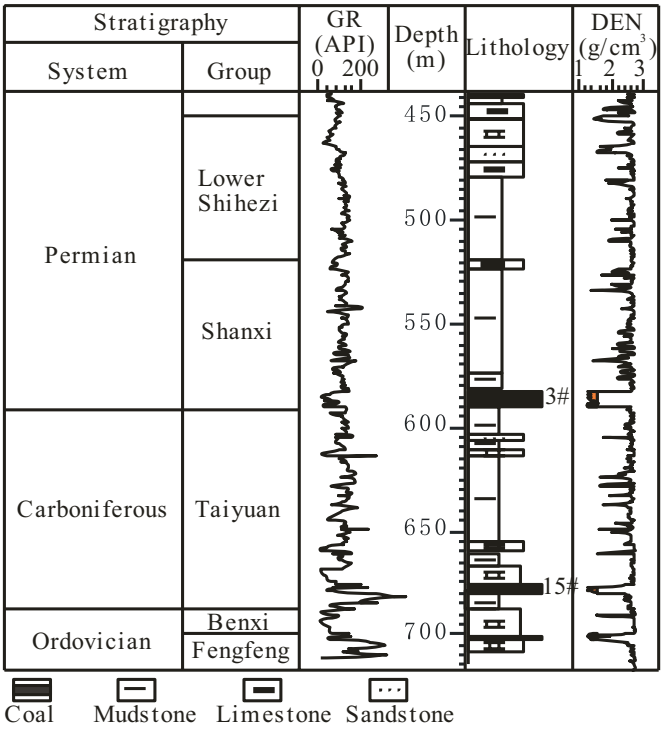

Figure 1. Stratigraphy of the study area (Zhou *et a*l., 2012).

No.3 in study area which belongs to the Shanxi groups. Burial depth at the top of coal seam No. 3 is deeper in west part than that in east part (Zhou *et al*., 2012). The average thickness of the seam is approximately 6 m. As of August 2011, there were 143 producers which produced from coal seam No.3. Considering the locations of the producers, they are history matched in 6 pilots separately (Figure 2).

2. METHODOLOGY

2.1. History matching

2.1.1. Basic data

History matching is carried out by adjusting the reservoir's uncertain parameters in a numerical reservoir model until the simulated well performances match the field history performance. This is an inverse process but the solution is not unique.

In Table 1, we list the parameters which can be adjusted during history matching and the uncertainty rank of these parameters. The ranking is based on parameters' heterogeneity, measurability, and effects on well performance. The history matching is completed by adjusting the porosity, permeability, skin factor, and coal mechanical parameters. Other data are fixed during history matchings.

The coal density, porosity and coal seam thickness are from the reservoir model presented in the paper by Zhou *et al*. (2012). The density is higher in the vicinity of

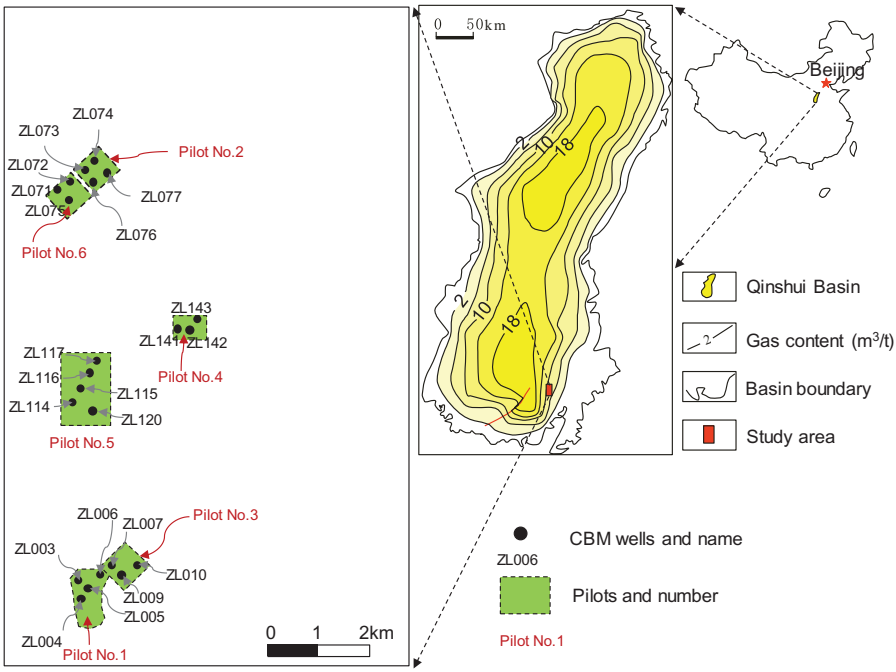

Figure 2. Location of study area and CBM wells and division of history matching pilots.

well ZL-006 because there is a well drilled in the Karst collapse (Wang *et al*., 1997; Zuo *et al*., 2009) column position. The coal fracture porosity ranges from 3.8-7.2% and the coal seam thickness ranges from 5.5-6.25 m (18-20.5 ft). The net gross ratio (N_{tg}) is calculated as –

$$N_{tg} = 100 - 88.36 \times \rho_{coal} + 114.21 \tag{1}$$

where ρ_{coal} is the coal density in g/cm^3. Table 2 shows the basic parameters in the model.

The initial reservoir pressure is assumed as the bore-hole opening pressure which is the pressure when the well was first opened to flow. We estimate the pressure distribution based on the bore-hole opening pressure of 50 wells using the convergent interpolation method (Bernstein, 1976; Zhou *et al*., 2012).

Figure 3 shows the distributions of density, coal seam thickness, net gross ratio and reservoir pressure.

Table 1. Uncertainty rank of the parameters in history matching (after Schlumberger, 2006).

Parameters	Spatial	Rank of uncertainty	Range
Porosity, ϕ	Local	Medium	0.1-10%*
Permeability, k	Local	High	0.001-50 mD*
Water saturation, S_w	Global	Low	
Langmuir isotherm	Global	Medium	
Net thickness, h	Local	Low	
Coal seam's top structure	Local	Low	
Coal density, ρ	Local	Medium	1.4-2.4 g/cm^{3**}
Horizontal permeability ratio, k_{hmax}/k_{hmin}	Global	Medium	1.0-17*
Ratio of vertical to horizontal permeability, k_v/k_h	Local	High	0.25-3*
Transmissibility	Local	High	
Fluid properties	Global	Low	
Coal shrinkage/ swelling coefficient	Global	High	0.27-2.83 kg/m^{3*}
Coal compressibility, c_p	Global	Low	1.31-29×10^{-5}kPa^{-1**}
Relative permeability, k_r	Global	High	
Initial reservoir pressure, p_o	Global	Low	
Initial gas saturation in face cleat, s_g	Global	Low	
Desorption time, τ	Global	Low	7-60 days**
Skin factor, s	Local	Medium	
Adsorption capacity	Local	Medium	2.8-22.6 m^3/t*
Young's Modulus, E	Global	Medium	0.85-6.1 GPa*
Poisson's ratio, v	Global	Medium	0.21-0.48*

Note: *from literature, ** from experimental data in the study area.

Table 2. Parameters used in the simulation models.

Reservoir property	Value	Conditions
Water viscosity, μ_w	0.89 cp	100 kPa, 25°C
Water density, ρ_w	1000 kg/m^3	100 kPa, 25°C
Gas specific gravity, γ (air=1)	0.68	100 kPa, 15°C*
Water compressibility, C_w	4.0×10^{-7} kPa^{-1}	
Water formation volume factor, FVF	1.0	100 kPa, 15°C*
Well radius, r_w	0.108 m	
Reservoir temperature, T	25°C	

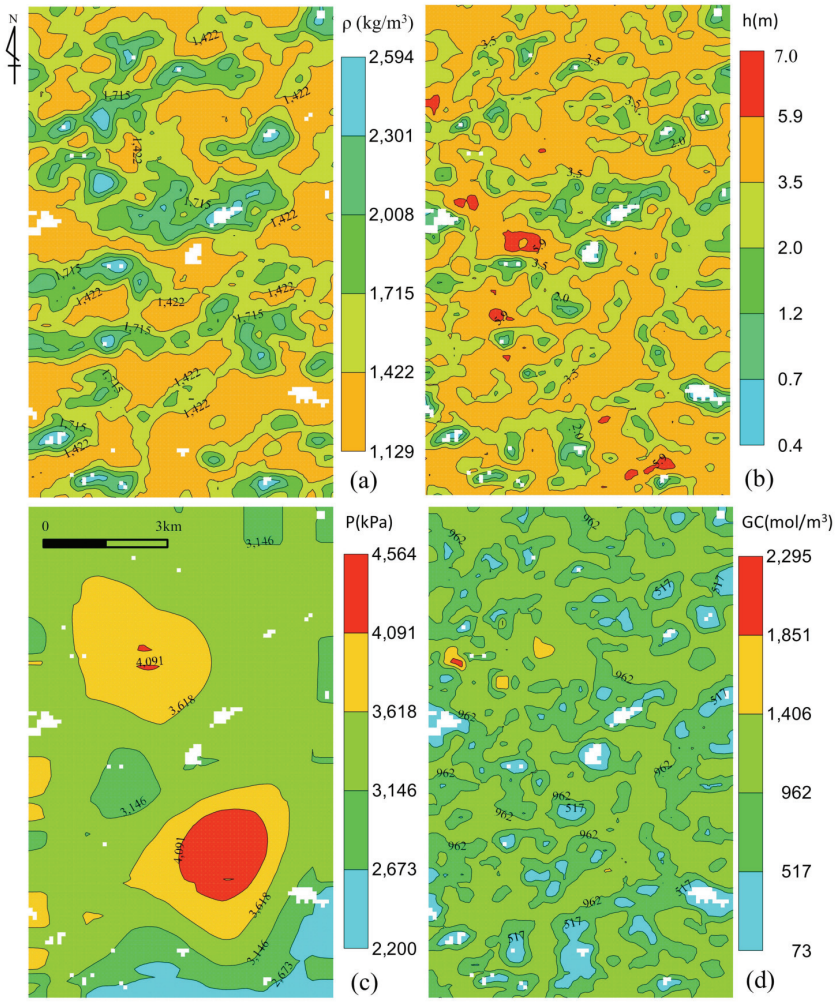

Figure 3. Propertiy distribution of coal seam No.3. (a) Density, (b) effective coal seam thickness, (c) initial reservoir pressure and (d) initial gas concentration (Zhou *et al*., 2013a).

2.1.2. Gas adsorption/desorption

We collected coal samples from the Duanshi Mine, a mine close to the study area, and carried out adsorption/desorption tests on them. We followed the procedure described by Yu *et al*. (2008). Before the tests, the coal samples were crushed to particle sizes ranging from 0.25 to 0.50 mm. Figure 4 shows the results of adsorption tests of CH_4 for one sample. The Langmuir volume and pressure are 767 kPa and 30.4 m^3/t, respectively (Zhou *et al*., 2013b).

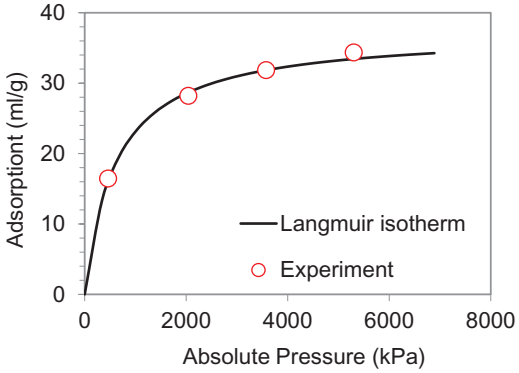

Figure 4. Experimental data and Langmuir isotherm curves on adsorption for one sample.

Desorption time is the required time to desorb 63.2% of the initial gas volume during a whole core desorption test. The sorption time for sample *i* is related to the shape factor and the diffusion coefficient using the following relationship –

$$\tau_i = \frac{1}{\sigma \cdot D_i} \tag{2}$$

where σ is the shape factor and D_i is the diffusion coefficient for sample *i*.

The desorption time, 25d, is used in the simulations. This is similar to the experimental average desorption time, 32d, of 62 samples. The σ and D_i are assigned with values of 0.01 and 4 m^2/day, respectively, to ensure that the desorption time is 25d.

2.1.3. Relative permeability

In CBM simulation, water and gas are assumed to be flow simultaneously when the gas saturation in the fracture is higher than the critical saturation. The flow rate of gas and water is affected by the relative permeability which varies within a wide range in the literature (Zhou 2012). The history matched results show that the Corey-type relative permeability (Figure 5) gave a good history match with an initial water saturation of 0.4, zero residual gas saturation, and a Corey exponent of 2.

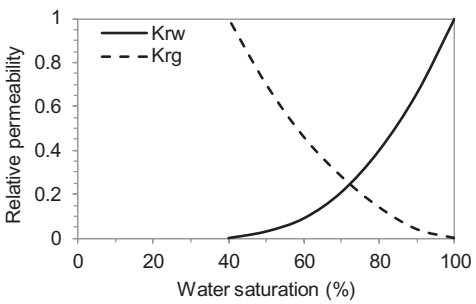

Figure 5. Gas-water relative permeability curves used in the simulations (Zhou, 2012).

2.2. Stochastic Simulation

2.2.1. Sequential Gaussian simulation

Stochastic simulations give multiple equal-probability realisations of reservoir properties based on the same input data. SGS is used in the analysis of hydrocarbon and CBM reservoir. SGS is a stochastic method based on kriging which honours well data, input distributions, variograms and trends. The variogram and distribution are used to create local variations, even those areas far away from the location of the input data. As a stochastic simulation, the result is dependent upon a random seed number. Multiple realisations are recommended to gain an understanding of uncertainty.

2.2.2. Cases and scenarios

Two cases with two different well spacings, 300 m (Case-1) and 2000 m (Case-2), are investigated and compared for simulations. There are 963 wells and 39 wells in Case-1 and Case-2 respectively. In each case, the 8 scenarios are used to study the effect of heterogeneity of coal permeability on CBM production. Figure 6 shows the eight settings for the heterogeneity of coal permeability variogram. The variogram type is exponential with nugget and sill equal 0 and 1, respectively. Scenarios No.1 through No.4 are used to compare the effect of major variogram direction and variogram range, while scenarios No.5 through No.8 are used to compare the effect of variogram range. These setting were also used to study their effects on estimation of coal resources by Zhou *et al*. (2012).

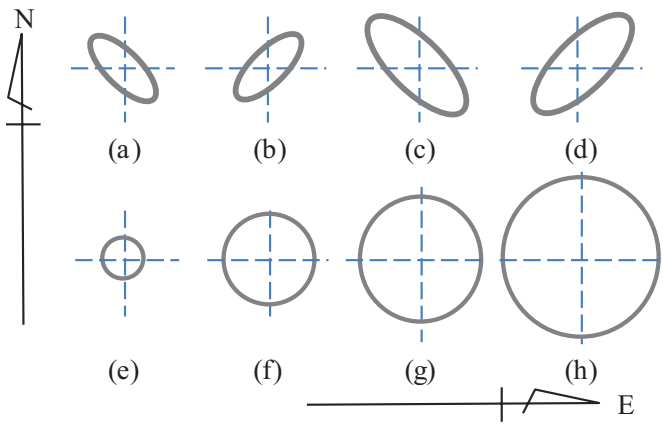

Figure 6. Setting for the heterogeneity of coal permeability variogram in facies (coal). (a) the major direction= 135°, the major range= 1300m, the minor range= 500m; (b) the major direction= 45°, the major range= 1300m, the minor range= 500m; (c) the major direction= 135°, the major range= 3000m, the minor range= 1000m; (d) the major direction= 45°, the major range= 3000m, the minor range= 1000m; (e) ranges in all directions= 500m; (f) ranges in all direction= 1300m; (g) ranges in all directions= 3000m; (h) ranges in all directions= 6000m. (Zhou et al., 2012)

3. RESULTS AND DISCUSSION

3.1. Porosity and permeability

We match the history of both gas and water production rates. Uncertain parameters, such as porosity, permeability and skin factor, were changed in history matching. We assume that coal in the study area has high shrinkage because its rank is anthracite. Table 3 shows the porosity multipliers and permeability of the 17 wells. The multipliers of porosity range from 0.2 to 1.3 and the permeabilities range from 1.5 to 12 mD. There are no descriptions of the porosity and permeability for the study area in literature, but there are many such descriptions for the Qinshui Basin (Table 4). The history matched porosity and permeability (Zhou *et al*., 2013a) are among those in literature.

Table 3. History matched porosity multipliers and permeabilities.

Well	Permeability, mD	Porosity multiplier
ZL-003	1.5	1.3
ZL-004	2.0	1.0
ZL-005	2.0	0.2
ZL-006	3.0	1.0
ZL-007	4.0	1.0
ZL-009	3.0	0.8
ZL-010	2.5	1.3
ZL-071	2.7	0.2
ZL-072	2.0	0.5
ZL-073	3.5	1.3
ZL-074	1.8	0.4
ZL-075	12.0	1.0
ZL-076	1.8	0.4
ZL-077	2.8	0.2
ZL-141	1.5	1.3
ZL-142	1.8	1.0
ZL-143	1.7	0.8
Mean	2.9	0.8

Table 4. History matched porosity and permeability in literature.

Literature	Study area	Porosity	Permeability, mD
Wu *et al*. (2011)	Panhe		0.65-2
Ye *et al*. (2011)	Panhe		0.15-2
Wong *et al*. (2007)	North Shizhuang	0.008	12.6
Liu *et al*. (2008)	Qinshui	0.06148	1.589
Chen *et al*. (2006)	Qinshui		0.5-6.66
Yang *et al*. (2010)	Qinshui	0.01-0.03	0.13-0.43
Yao *et al*. (2007)	Pingdingshan	0.04-0.10	0.806-27.7

3.2. Formation damage

Figure 7 shows the skin factors of nine wells while other eight wells used zero skin factors in history matching. Initially, only well No.ZL010 has a positive skin factor of 3 but mitigate to zero on day 351. Wells No.ZL005, No.ZL008, No.ZL007 and No.ZL071 have positive skin factors from day 139, 240, 212 and 212, respectively.

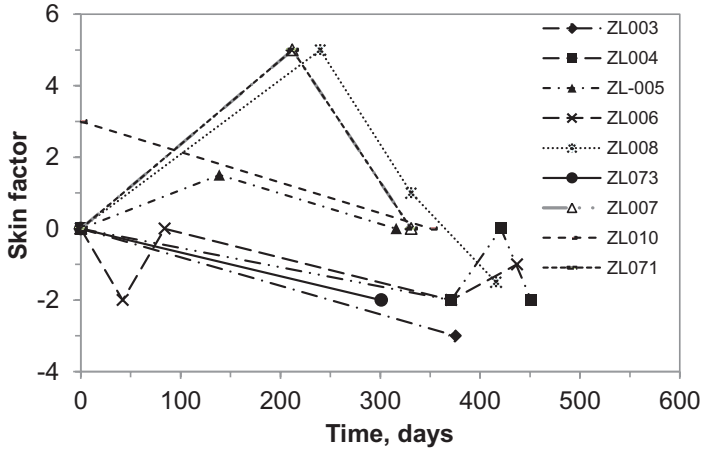

Figure 7. Skin factor used in history matching.

3.3. Distribution of coal permeability

Figure 8 shows the porosity distribution which was used in simulations. The porosity was populated by combining the log interpreted porosity and the history matched porosity

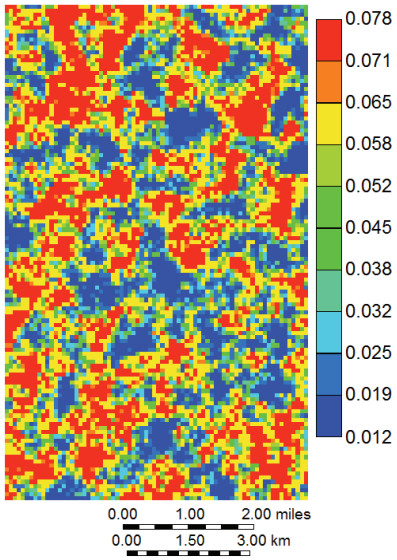

Figure 8. Porosity distribution used in simulations.

multipliers using interpolating method. It can be seen from Figure 8 that the porosity in the study area ranges from 1.2% to 7.8%.

Figure 9 shows one realisation of coal permeability of each scenario in Case-1. Obviously, the permeability distributions are continuous along the major directions of histogram, and longer variogram range yields more continuous distribution of permeability.

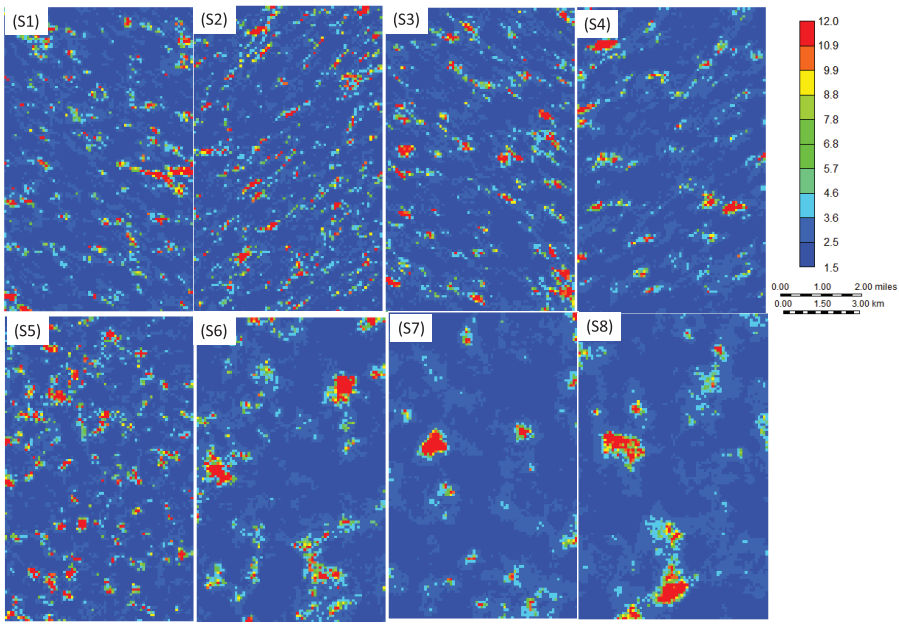

Figure 9. One realisation of coal permeability for the eight scenarios in Case-1.

3.4. CBM production

Eight different heterogeneous scenarios for coal permeability are simulated based on the same coal seam thickness, porosity and coal density, etc. Figure 10 shows the cumulative gas productions of the eight scenarios of Case-1. Each scenario has 20 simulations based on 20 realisations of coal permeability using SGS. Results show that scenarios No.1 through No.5 have similar concentrated cumulative gas production curves. However, scenarios No.6 and No.7 have wider distributed curves and that of scenario No.8 is the widest. It means that the major direction of variogram has less effect on the uncertainty of CBM production than variogram range when the well spacing is 300 m.

Figure 11 shows the cumulative gas productions of eight scenarios of Case-2. Each scenario has also 20 simulations based on 20 realisations of coal permeability using SGS. Results show that scenarios No.3, No.4, No.6, No.7 and No.8 have similar concentrated distributed cumulative gas production curves. However, scenarios No.1, No.2 and No.5 have wider distributed curves. It means that the major direction of

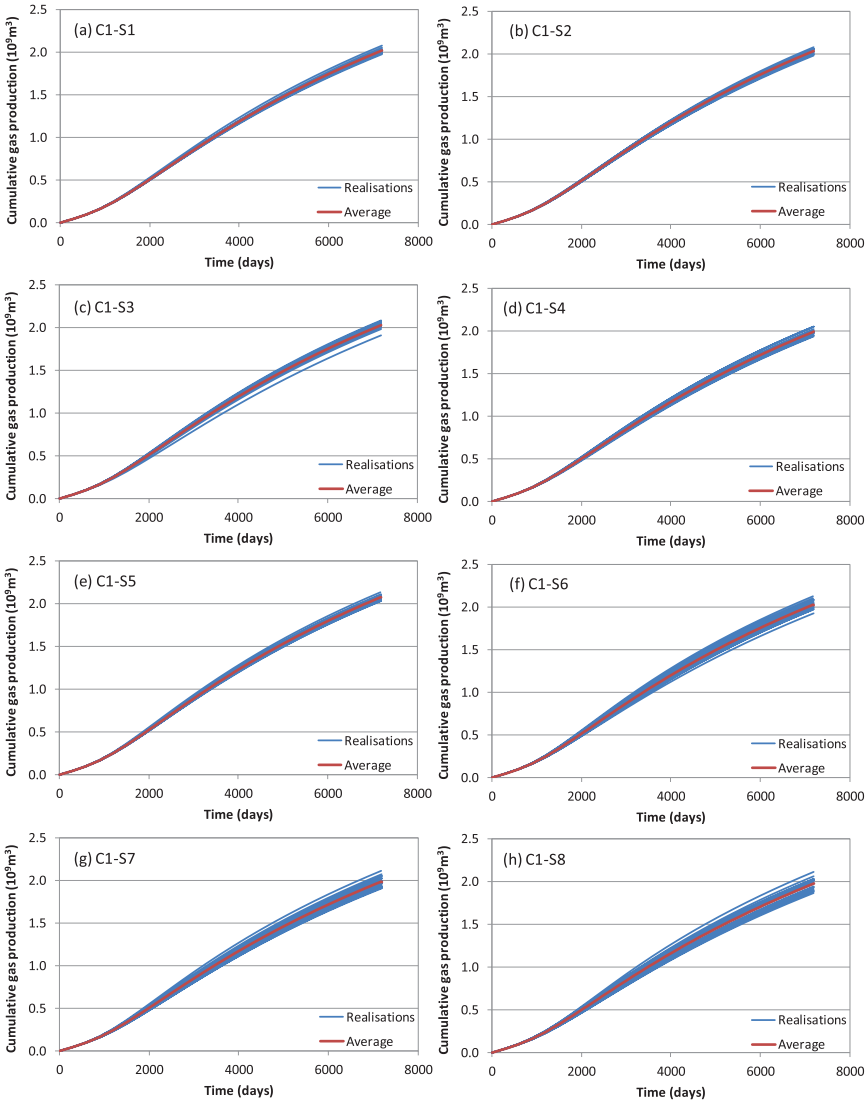

Figure 10. Comparisons of cumulative gas production for eight scenarios of 20 realisations of coal permeability of Case-1.

variogram also has less effect on the uncertainty of CBM production than variogram range when the well spacing is 2000 m. It is noteworthy that the effects of variogram range on the uncertainty of CBM production is positive for Case-1 and vice versa for Case-2.

Figure 12 shows the average cumulative gas production for the 16 scenarios in Case-1 and Case-2. For Case-1, scenario-5 has the highest cumulative CBM

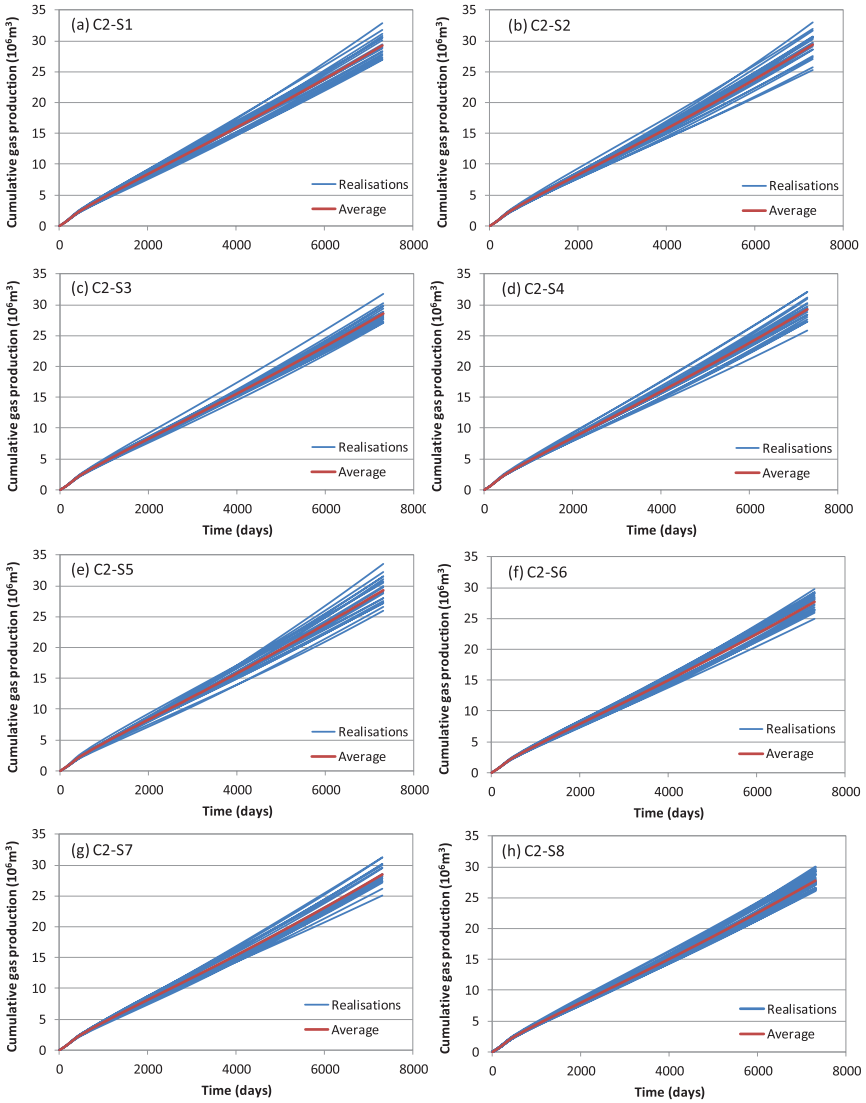

Figure 11. Comparisons of cumulative gas production for eight scenarios of 20 realisations of coal permeability of Case-2.

production ($2.077\times10^9 m^3$) (Figure 12a). The average cumulative gas productions decrease from scenario No.5 to No.8 with the increase in variogram range. Scenarios No.3 and No.4 have lower average cumulative gas productions than scenarios No.3 and No.4 because the variogram range of the former is bigger than the later (Figure 12a).

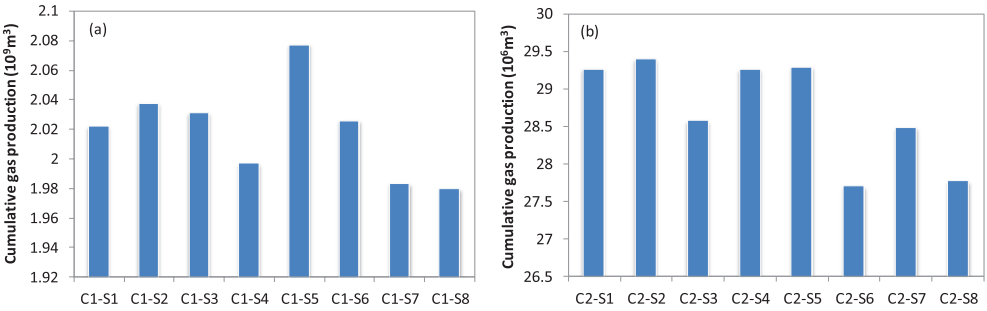

Figure 12. Comparisons of average cumulative gas production for eight scenarios of (a) Case-1 and (b) Case-2.

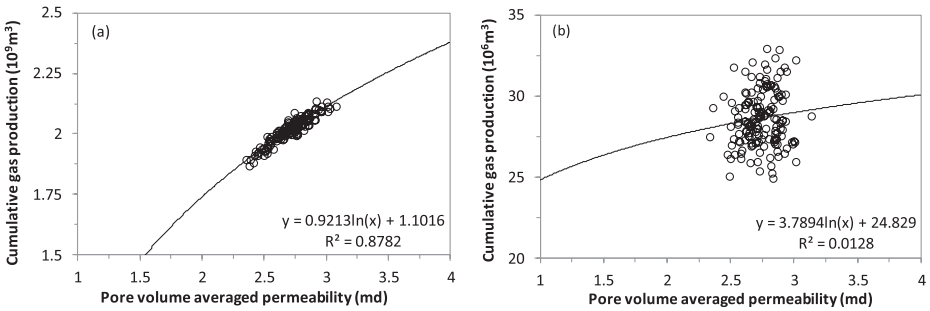

Figure 13. Relationship between cumulative gas production of all simulations and the pore volume-averaged permeability in (a) Case-1 and (b) Case-2.

For Case-2, scenario No.2 has the highest cumulative CBM production (29.391×10^6m^3) while scenario No.6 has the lowest one (27.705×10^6m^3) (Figure 12b). There is no obviously trend between the cumulative gas production and the pore-volume averaged permeability in this case.

Figure 13 shows the relationship between the cumulative gas production of all simulations and the pore-volume averaged permeabilities. The relationship is strong for Case-1 (Figure 13a) while scattered for Case-2 (Figure 13b). This is because the 963 wells are distributed closely and the cumulative gas production is directly dominated by the pore-volume averaged permeability in Case-1. However, the cumulative gas production of the 39 wells in Case-2 are scattered which are contributed by local permeability not by the pore-volume averaged permeability of the whole reservoir.

4. CONCLUSIONS

This paper has a novel study for the effect of variogram on CBM production based on the history matched permeabilities in a CBM field in Qinshui Basin, China. Two cases with different well spacing and eight scenarios with different major variogram

directions and variogram ranges in each case are simulated for CBM production. Following conclusions are drawn –

1. The history matched porosities range from 1.2% to 7.8% and the permeabilities ranges from 1.5 mD to 12 mD.
2. The major direction of variogram has less effect on the uncertainty of CBM production than variogram range for both cases with well spacings of 300 m and 2000 m.
3. The effects of variogram range on the uncertainty of CBM production are positive for the case with well spacing of 300 m and vice versa for the case with well spacing of 2000 m.

ACKNOWLEDGEMENTS

This work was partially carried out in the context of the China-Australia Joint Coordination R&D Grants supported by the Department of Resources, Energy and Tourism, Australia. The authors also acknowledge the support of Fundamental Research Funds for the Central Universities, China University of Geosciences (Wuhan) (CUGL100249). We also thank the China United CBM Co. for the permission to publish the paper.

REFERENCES

Beretta F.S., Costa J.F. and Koppe J.C., 2010. Reducing coal quality attributes variability using properly designed blending piles helped by geostatistical simulation. *International Journal of Coal Geology* **84**, 83-93.

Bernstein R., 1976. Digital image processing of earth observation sensor data. *IBM Journal of Research and Development* **20(1)**, 40–57.

Cairncross B. and Cadle A.B., 1988. Paleoenvironmental control on coal formation, distribution and quality in the Permian Vryheid formation, East Witbank Coalfield, South Africa. *International Journal of Coal Geology* **9**, 343-370.

Chen J. Qin Y. and Fu X., 2006. Numerical Simulation on dynamic variation of the permeability of high rank coal reservoirs during gas recovery. *Journal of China University of Mining &Technology* **35 (1)**, 49-53. (In Chinese with English abstract).

Ding S.L., Liu J.J. and Xu B.H, 2012. Factors influencing coal bed methane reservoir in southeastern edge of Ordos Basin, China. *Energy Exploration and Exploitation* **30(4)**, 677-688.

Hagelskamp H.H., Eriksson P.G. and Snyman C.P., 1988. The effect of depositional environment on coal distribution and quality parameters in a portion of the Highveld coalfield, South Africa. *International Journal of Coal Geology* **10**, 51-77.

Heriawan M.N. and Koike K., 2008. Identifying spatial heterogeneity of coal resource quality in identifying spatial heterogeneity of coal resource quality in a multilayer coal deposit by multivariate geostatistics. *International Journal of Coal Geology* **73**, 307-330.

Hindistan A.M., Tercan E.A. and Ünver B., 2010. Geostatistical coal quality control in Longwall mining. *International Journal of Coal Geology* **81**, 139-150.

Jakeman L.B., 1980. The relationship between formation structure and thickness in the Permo-Triassic succession of the Southern coalfield, Sydney Basin, New South Wales, Australia. *Mathematical Geology* **12**, 185-212.

Keim S.A., Luxbacher K.D. and Karmis M., 2011. A numerical study on optimization of multilateral horizontal wellbore patterns for coalbed methane production in Southern Shanxi Province, China. *International Journal of Coal Geology* **86**, 306-317.

Liu R., Liu F., Zhou W., Li J. and Wang H., 2008. An analysis of factors affecting single well deliverability of coalbed methane in the Qinshui Basin. *Natural Gas Industry* **28(7)**, 30-33. (In Chinese with English abstract)

Liu G., Zheng L., Gao L., Zhang H. and Peng Z., 2005. The characterization of coal quality from the Jining Coalfield. *Energy* **30**, 1903-1914.

Lv Y., Tang D., Xu H. and Luo H., 2012. Production characteristics and the key factors in high-rank coalbed methane fields: A case study on the Fanzhuang Block, Southern Qinshui Basin, China. *International Journal of Coal Geology* **96-97**, 93-108.

Mastalerz M. and Kenneth R.W., 1994. Variations in SEAM thickness, coal type and coal quality in the Namurian succession of the Intrasudetic basin (south western Poland). *Palaeogeography, Paleoclimatology, Palaeoecology* **106**, 157-169.

Schlumberger, 2006. Reservoir simulation application training course and (Eclipse) workshop, SIS training and development, Denver and Houston. *http://www.fanarco.net/books/reservoir/simulation/ARS-Day2_HM_3_of_3.pdf*, viewed on 26th July 2013.

Stevens S.H., Spector D. and Riemer P., 1998. Enhanced coalbed methane recovery using CO_2 injection: Worldwide resource and CO_2 sequestration potential. *SPE Paper 48881*, presented at SPE International Oil and Gas Conference and Exhibition in China, Beijing, China.

Wang H., Li Y., Wang E. and Zhao Z., 1997. Strategic ground water management for the reduction of karst land collapse hazard in Tangshan, China. *Engineering Geology* **48**, 135-148.

Wong S., Law D., Deng X., Robinson J., Kadatz B., William D.G., Ye J., Feng S. and Fan Z., 2007. Enhanced coalbed methane and CO_2 storage in anthracitic coals-Micro-pilot test at South Qinshui, Shanxi, China. *International Journal of Greenhouse Gas Control* **1**, 215-222.

Wu J., Sun M., Feng S., Guo B., Ye J. and Fan H., 2011. Good lessons from the state level demonstration project of coalbed methane development: An overview of such high tech and commercial project in the southern Qinshui Basin. *Natural Gas Industry* **31(5)**, 9-15. (In Chinese with English abstract)

Ye J., Zhang J. and Wang Z., 2011. Production performance and its controlling factors in the Panhe CMB Gas Field, southern Qinshui Basin. *Natural Gas Industry* **31(5),** 28-30. (In Chinese with English abstract)

Yu H., Zhou L., Guo W., Cheng J. and Hu Q., 2008. Predictions of the adsorption equilibrium of methane/carbon dioxide binary gas on coals using Langmuir and

ideal adsorbed solution theory under feed gas conditions. *International Journal of Coal Geology* **73**, 115-129.

Zhou F., 2012. Integrated history matching of a complex performance horizontal well and prediction for coalbed methane production. *Journal of Petroleum Science and Engineering* **96-97**, 22-36.

Zhou F., Allinson G., Wang J., Sun Q., Xiong D. and Cinar Y., 2012. Stochastic modelling of coalbed methane resources: A case study in Southeast Qinshui Basin, China. *International Journal of Coal Geology* **99**, 16-26.

Zhou F., Hou W., Allinson G., Cinar Y., Wu J., Wang J., 2013a. A feasibility study of ECBM recovery and CO storage for a producing CBM field in Southeast Qinshui Basin, China. *International Journal of Greenhouse Gas Control* **19**, 26-40.

Zhou F., Hussain F., Guo Z., Yanici S. and Cinar Y., 2013b. Adsorption/ desorption characteristics for methane, nitrogen and carbon dioxide of coal samples from Southeast Qinshui Basin, China. *Energy Exploration & Exploitation* **31(4)**, 645-665.

Zuo J., Peng S., Li Y., Chen Z. and Xie H., 2009. Investigation of karst collapse based on 3-D seismic technique and DDA method at Xieqiao coal mine, China. *International Journal of Coal Geology* **78**, 276-287.